

LINEAR AND NONLINEAR MODELING FOR AN ELECTRONIC THROTTLE BODY

**Eric Teuscher¹, Benedikt Alt¹, Ferdinand Svaricek¹,
Jan Peter Blath², Matthias Schultalbers²**

¹University of the German Armed Forces, Department of Aeronautical Engineering
Institute of System Dynamics and Flight Mechanics, 85577 Neubiberg, Germany

²Department of Powertrain Mechatronics, Development Gasoline Engines at IAV GmbH,
38518 Gifhorn, Germany

Benedikt.alt@unibw.de (Benedikt Alt)

Abstract

An electronic throttle body is an important part of the automotive powertrain of modern passenger vehicles with spark ignition engines. This component should regulate the air mass flow into the intake manifold of the engine. A precise control of the throttle plate position is critical to drivability, fuel economy and to fulfill strict emission constraints. Cost, material and packaging regulations of the automotive industry let the throttle open-loop dynamics become rather complex, exhibiting numerous nonlinearities like e.g. friction and limp-home effects. Furthermore, nonlinear effects of the electronic throttle's electric drive augment this complexity again. Hence, the design for the position controller of the throttle plate becomes difficult and robust model-based control design strategies have to be applied. The aim of this paper is to give an overview of modeling approaches for an electronic throttle body. With a validated simulation model it would be much easier to develop a robust position controller for the throttle plate. This could be used as an inner loop in a complex control framework of an engine electronic control unit of a modern passenger vehicle. For the electronic throttle body several modeling approaches are discussed and compared. Hereby the main focus lies on an exact model description of the electric drive, the spring mechanism and the friction torques. The resulting simulation models are validated on a test rig and conclusions are drawn.

Keywords: Automotive applications, electronic throttle, permanent magnet actuator, friction modeling, limp-home effects

Presenting Author's Biography

Benedikt Alt received his diploma in aeronautical engineering and space technology from the University of Stuttgart, Stuttgart, Germany in 2005. Since 2006 he works as a research assistant in the control engineering group at the Department of Aeronautical Engineering at the University of the German Armed Forces, Munich, Germany. His research interests are modeling challenges for automotive and mechatronic applications and nonlinear and robust control design methods. Especially, his interest tends to sliding mode control theory.



1 Introduction

In the past the driver's pedal was linked mechanically to the throttle plate and hence the air mass flow into the intake manifold was regulated rather imprecisely and the fuel consumption and emissions were often to high. Due to the sluggish dynamic behaviour of the intake manifold the driveability was additionally quite low. Thus, it was important that modern control strategies were developed that can optimize the aforementioned engine characteristics. In this context it is well known that modern electronic control unit's (ECU) functional architecture is characterized by a centrally coordinated torque management [1]. This means that engine torque represents the central system variable and all torque demands result in a variation of torque and are defined on this basis. In this new strategy the driver's pedal position is interpreted as a command signal to this new 'drive-by-wire' system (Figure 1).

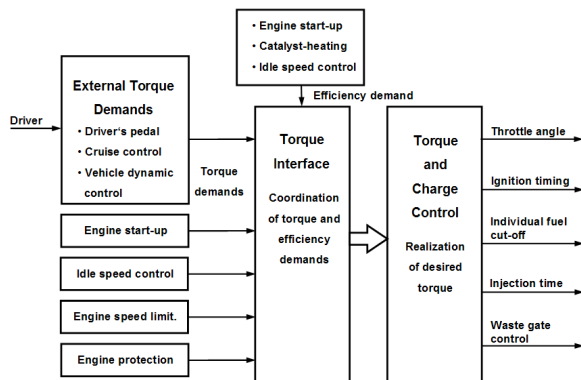


Fig. 1 Torque management of a modern passenger vehicle's engine control unit

The assumption to this new control strategy and all its benefits on engine and vehicle level is the ensuement of a fast and accurate inner loop throttle position control. With this, the electronic throttle body became a very important component of the automotive powertrain of modern passenger vehicles. Cost, material and packaging constraints of the automotive industry often lead to rather simple and low-cost constructions of the electronic throttle body. On the other hand, the throttle open-loop dynamics become rather complex. Especially, dependencies on temperature, humidity and aging effects grow up rapidly with the use of low-cost automotive components. Furthermore, numerous nonlinearities like e.g. friction and limp-home effects influence the throttle open-loop dynamics as well. Hence, the design of a precise position control for the throttle plate is more and more challenging.

The existing control schemes for the electronic throttle body are mostly based on PID controllers. This is mainly because (i) they are capable of controlling this process, maybe not as optimally as one would have ideally liked, but are nominally doing the job, (ii) they are easy to implement, integrate, service and replace and

(iii) more important they are cost-effective. Due to the recent advances in the electronics sector, it is now possible to implement high-level logical operations on the engine's electronic control unit and more sophisticated controllers are able to do the control-job in a more efficient and optimal manner. Thus, electronic throttle control is an interesting area for the application of robust control design strategies. In [2] a flatness based controller is used for the electronic throttle control. In [3] a self-tuning control strategy is developed and in [4] an adaptive pulse control is introduced. Furthermore, electronic throttle control is an interesting application for variable structure control [5, 6] or sliding mode control strategies [7, 8, 9, 10]. In [11] an adaptive sliding surface controller is adopted to the electronic throttle body.

Many of the aforementioned control strategies need a state-space model of the electronic throttle body's behaviour. Furthermore, these control strategies are usually developed and tested using an extended simulation model. Hence, a detailed simulation model of the electronic throttle body has to be built. Thus, modeling of the electronic throttle body is still an interesting area for research, although numerous works have already been presented during the last decades. On the one hand, there exist many control orientated modeling approaches that often lead to linear state-space models that can also be used for control design strategies [5, 12]. On the other hand, some authors include the friction and limp-home effects in their modeling approaches [13, 14]. In the literature of the electrical research engineers, there exist also extended nonlinear models of the electric drive of the electronic throttle body [15]. The aim of this paper is to show different modeling approaches for a special design of an electronic throttle body. These approaches with some problems, that have arisen during the modeling and possible strategies of solution will be addressed in this paper.

The remainder of the paper is organized as follows: Section 2 introduces the relevant notation for the modeling approaches of the electronic throttle body. In section 3 the design of the electronic throttle body is explained. Section 4 considers several modeling approaches for the electric drive. In section 5 several modeling approaches for the mechanical subsystem are given including the spring mechanism, the limp-home effects and the mathematical description of the friction effects. The approaches for the overall model description of the electronic throttle body are discussed in section 6. Additionally, a comparison to experimental results is given in section 7. Finally, conclusions are drawn in section 8 and an overview of future work is given.

2 Notation

b	Width of the coil [m]
b_{Fe}	Iron width inside the coil [m]
B	Magnetic flux density [Vs/m ²]
B_R	Remanence, residual magnetism [Vs/m ²]

c_M	Electric drive constant [Nm/A]
d	Diameter of the spring wire [m]
D	Diameter of the torsion spring [m]
E	Elasticity modulus [N/mm ²]
G	Weight [N]
h	Height of the coil [m]
H	Magnetic field intensity [A/m]
i	Electric current [A]
J	Moment of inertia [kgm ²]
L	Inductivity [H]
l_A	Length of the electric flux line (armature) [m]
l	Length of the lever arm [m]
l_{Fe}	Iron length inside the coil [m]
N	Number of ampere-turns of the coil [-]
n	Number of turns of the spring [-]
P	Power rating [W]
R	Resistance [Ω]
R_F	Constant of the torsion spring [Nm/degree]
r_1	Radius of the armature [m]
T	Time constant [s]
T_c	Dynamic friction torque [Nm]
T_{el}	Electric torque [Nm]
T_f	Friction torque [Nm]
T_{mech}	Mechanical torque [Nm]
T_s	Static friction torque [Nm]
T_{sp}	Spring torque [Nm]
T_{Thr}	Overall Torque [Nm]
u_{SP}	Input voltage [V]
m	Mass of the throttle plate [kg]
β	Opening angle of the iron yoke [degree]
δ	Air gap [m]
ϕ_{thr}	Throttle plate position [degree]
$\dot{\phi}_{thr}$	Throttle plate velocity [degree/s]
γ	Measurement angle [degree]
μ	Permeability [kgm/(A ² s ²)]
Ψ	Magnetic flux [Vs]
$\hat{\Psi}$	Magnetic flux at ϕ_{max} [Vs]
ω_m	Throttle plate velocity [degree/s]

3 Design of the electronic throttle body

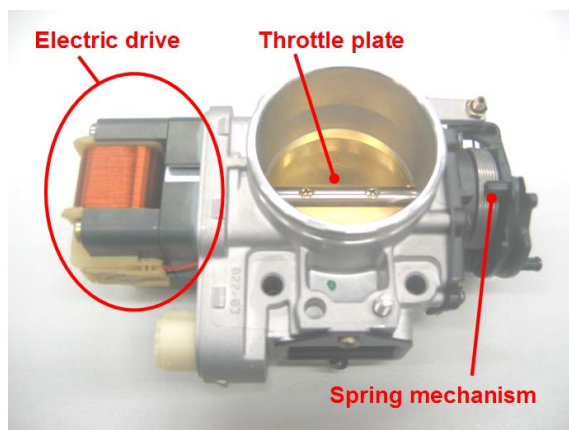


Fig. 2 Electronic throttle body

An electronic throttle body consists of two subsystems. The electrical subsystem produces the electric torque

$T_{el} = h(u_{SP})$ and the mechanical subsystem dissipates the mechanical torque $T_{mech} = f(\phi, \dot{\phi})$ that includes the spring torque T_{sp} , the friction and the limp-home effects. The overall torque T_{thr} results from

$$T_{thr} = T_{el} - T_{mech}. \quad (1)$$

In section 4 several modeling approaches for the unknown electric torque $T_{el} = h(u_{SP})$ are introduced and in section 5 some mathematical descriptions for the mechanical subsystem $T_{mech} = f(\phi, \dot{\phi})$ are presented. As a start the design of the electrical and mechanical subsystems of the underlying electronic throttle body (Figure 2) is explained.

3.1 Design of the electrical subsystem

For an electronic throttle plate a rotational movement of up to 90 degrees is required. The standard design for the electric drive of an electronic throttle body is a brushed DC-motor with gear box. Nevertheless, there exist some alternatives in order to simplify the design of such an electrical subsystem. One of these ideas is the permanent magnet actuator. A diametrically magnetized cylindrical solenoid rotates inside an iron yoke (Figure 3). The magnet is driven by a magnetic coil. A current i flows through this inductivity L when an input voltage u_{SP} is applied and a magnetic field arises. Hence, the permanent magnet starts to rotate and to generate the electric torque T_{el} .

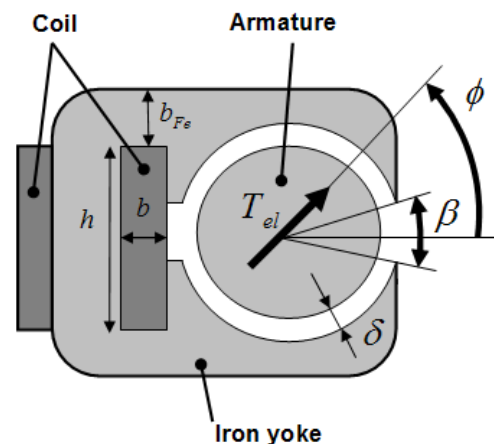


Fig. 3 Principle sketch of the permanent magnet actuator of the electric drive

3.2 Design of the mechanical subsystem

The body of the electronic throttle comprises a suction pipe connecting the air filter to the intake manifold. In the middle of this pipe a throttle plate is mounted on a pivoted shaft. The aforementioned electric drive on the same shaft allows the throttle plate to rotate up to 90 degrees (until its stop position). Thus, the air mass can flow directly into the intake manifold. A mechanism of torsion springs returns the throttle plate into its idle state if the electric drive is switched off.

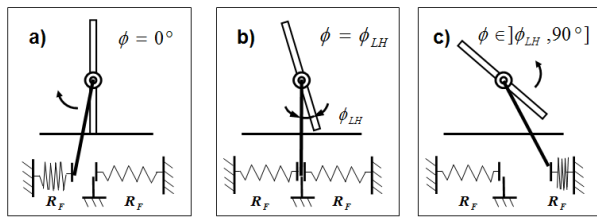


Fig. 4 Principle sketch of the spring mechanism. a) Throttle plate in closed position, b) throttle plate in Limp-Home position and c) throttle plate in open position

The principle sketch of this spring mechanism is illustrated in Figure 4. It is shown that two springs hold the throttle plate in its idle state, the so called limp-home position, where the throttle is slightly opened ($\phi_{LH} = 3$ degrees). Thus, a possible engine stall is prevented in case of an electric drive failure. If the throttle plate is moved out of this limp-home position by the electric drive - either in positive or negative direction - a spring torque T_{sp} is directed against this electric torque and it returns the throttle plate to its limp-home position if the electric torque is removed. Beside this spring torque T_{sp} , there exists severe friction both in the bearing and in the spring torque mechanism of the mechanical subsystem. Hence, it is a challenging task to find a mathematical description for the prescribed electronic throttle body that comprises all the aforementioned physical effects. In section 5 different modeling approaches are shown and discussed.

4 Models for the electrical subsystem

In this section different modeling approaches for the electrical subsystem are introduced.

4.1 Linear model for the electric drive

Often, the linear relationship

$$T_{el}(t) = c_M i(t) . \quad (2)$$

is used to describe the generation of the electric torque T_{el} . As the current $i(t)$ is an internal model state and the voltage u_{SP} is the input to the electronic throttle body a relationship for the current $i(t) = h_1(u_{SP})$ is required. This electric circuit can be described as a series connection of a resistance R and an inductivity L .

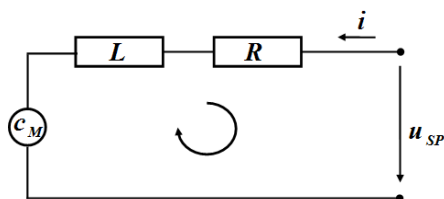


Fig. 5 Block diagram for the electric drive of the electronic throttle body

Additionally, an armature reaction $c_M \dot{\phi}$ leads to a self-induction effect. Thus, the well-known Kirchhoff's law can be applied:

$$u_{SP} - L \frac{di(t)}{dt} - Ri(t) + c_M \dot{\phi} = 0 . \quad (3)$$

In this linear approach it is assumed that the value for the resistance R is a constant parameter with $R = 1.25\Omega$. The inductivity L should also be constant with $L = 0.02$ H.

What remains to do is the identification of the electric drive constant c_M . This model parameter can be identified from the measured torque T_{el} with varying current i . It can be shown that for a given throttle plate position there exists nearly a linear relationship. The electric drive constant represents a mean value slope of such characteristics for different throttle plate positions.

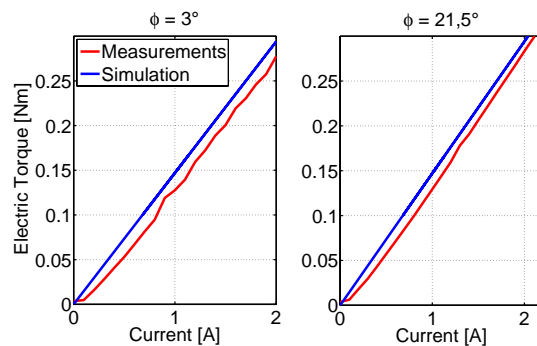


Fig. 6 Electric torque over current for two different throttle plate positions

In Figure 6 the characteristics for two different throttle plate positions are shown. The resulting electric drive constant is taken to $c_M = 0.132$ Nm/A. For more information about this modeling approach the reader is referred to [12].

4.2 Nonlinear model for the electric drive

The next model of the electric drive is an extension of the approach of Section 4.1. This extended approach considers the value of the inductivity L not to remain constant. It is assumed that there exists the following

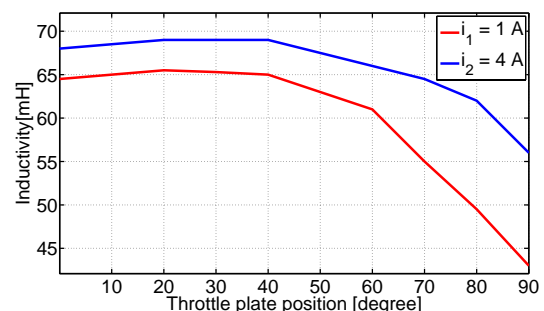


Fig. 7 Characteristic for the nonlinear inductivity

nonlinear relationship:

$$L = h_2(i, \phi). \quad (4)$$

The resulting nonlinear characteristic of equation (4) is identified experimentally and illustrated in Figure 7. The remaining part of the second modeling approach for the electric drive is similar to the first model. In Section 4.3 an extended nonlinear modeling approach for the electric drive is given.

4.3 Extended nonlinear model for the electric drive

In this section an extended nonlinear modeling approach for the torque generation of the electric drive is considered. From [15] it can be deduced that the electric torque T_{el} of the permanent magnet actuator can be calculated from the following relationship:

$$T_{el}(\phi) = Ni \left. \frac{\partial \Psi(\phi)}{\partial \phi} \right|_{i=0} \quad (5)$$

with N the number of ampere-turns and $\Psi(\phi)$ the magnetic flux as a function of the throttle position ϕ . Figure 3 shows that the following relationship for the magnetic flux $\Psi(\phi)$ holds true:

$$\Psi(\phi) = \hat{\Psi} \sin(\phi). \quad (6)$$

For the calculation of the amplitude of the magnetic flux $\hat{\Psi}$ it is assumed that the throttle plate position is opened at $\phi = 90$ degrees. From [15] it is also known that $\hat{\Psi}$ can now be calculated by:

$$\hat{\Psi} = l_A \int_{\beta/2}^{\pi-\beta/2} B_\delta(\phi) r_1 d\phi \quad (7)$$

with $B_\delta(\phi)$ the radial component of the flux density in the air-gap. Under the assumption of $\mu_{Fe} \rightarrow \infty$ this unknown flux density can be calculated from

$$\oint \vec{H} d\vec{l} = H_A(\phi) l_A(\phi) + H_\delta(\phi) 2\delta = 0 \quad (8)$$

where

$$l_A(\phi) = 2r_1 \sin(\phi) \quad (9)$$

with r_1 the inner radius of the armature. From [15] the magnetic field intensity H_A of the permanent magnet actuator is known as

$$H_A = \frac{B_A - B_R}{\mu_0 \mu_A} \quad (10)$$

with B_R the magnetic remanence. Furthermore, the width of the air-gap δ is assumed so small that the entire magnet flux is conducted in the iron:

$$B_A(\phi) \approx B_\delta(\phi). \quad (11)$$

Hence, a nonlinear relationship for the unknown radial flux component of the air-gap B_δ of equation (7) is

found and the amplitude of the flux $\hat{\Psi}$ in the air-gap δ can now be calculated by

$$\hat{\Psi} = 2B_R r_1 l_{Fe} \int_{\beta/2}^{\pi/2} \frac{1}{\sin(\phi) + \mu_A \frac{\delta}{r_1}} \sin(\phi) d\phi. \quad (12)$$

Although an exact solution of equation (12) is possible, it is advisable to use an approximation for this integral.

Tab. 1 Parameters for the extended nonlinear electric drive model

Parameter	Value	Description
N	238	Number of ampere-turns [-]
B_R	1.3	Remanence [Vs/m ²]
r_1	0.014	Radius of the armature [m]
δ	0.0004	Air gap [m]
μ	360	Permeability [kg m/(A ² s ²)]
β	17	Yoke position [degree]
l_{Fe}	0.12	Iron length inside the coil [m]

Different simplifications for this problem are listed and compared in [15]. In the case of the considered electronic throttle body the following approximation for the amplitude of the flux $\hat{\Psi}$ has shown reasonable results:

$$\hat{\Psi} = 2B_R r_1 l_{Fe} \frac{1}{\sin(\frac{1}{2}(\frac{\pi}{2} + \frac{\beta}{2})) + \frac{\delta}{r_1} \mu_A} \cos(\frac{\beta}{2}). \quad (13)$$

Finally, the electric torque of the electronic throttle body can be calculated by

$$T_{el} = 2NiB_R r_1 l_{Fe} \frac{1}{\sin(\frac{1}{2}(\frac{\pi}{2} + \frac{\beta}{2})) + \frac{\delta}{r_1} \mu_A} \cos(\frac{\beta}{2}) \cos(\phi). \quad (14)$$

The physical parameters of equation (14) are listed in Table 1.

4.4 Validation of the electric drive models

In this section the modeling approaches of sections 4.1, 4.2 and 4.3 are compared. Therefore, an input voltage $u_{sp} = 1.5$ V is applied to the electrical subsystem in the simulation and the corresponding output is the electric torque T_{el} .

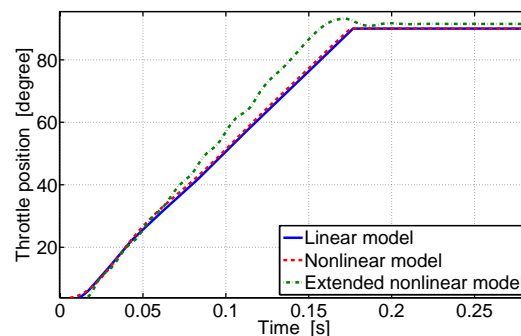


Fig. 8 Validation of the modeling approaches for the electrical subsystem

The corresponding values of the throttle position $\phi(t)$ can be obtained by solving the simple differential equation

$$J\ddot{\phi} = T_{el} \quad (15)$$

under the assumption that the moment of inertia J is known. Figure 8 shows the simulation results. It is emphasized that the output ϕ of the simulation models of sections 4.1 and 4.2 is in both cases limited at 90 degrees. The output of the simulation model of section 4.3 doesn't need these limitations because it includes the saturation effect of the permanent magnet actuator itself.

It can be seen from Figure 8 that there is an acceptable accordance between the prescribed linear and nonlinear modeling approaches in this case. The extended nonlinear modeling approach shows a different opening characteristic for the throttle plate. Especially for throttle plate angles greater than 30 degrees the electric torque arises obviously more and the throttle plate opens faster. This deviation comes from the following simplification: In the extended nonlinear simulation model for the electric drive the non-magnetic shaft inside the armature is not taken into consideration. Instead it is assumed that the armature consists completely of the same iron material. By this assumption the resulting torque T_{el} in the simulation should be increased compared to the measurements. In Figure 8 it can be seen that the prescribed deviation really exists, but it seems to be relatively small. Hence, in this first approach the effect of the non-magnetic shaft inside the armature is neglected in the remainder of this paper.

5 Models for the mechanical subsystem

In this section different modeling approaches for the mechanical subsystem are introduced.

5.1 Linear model for the mechanical subsystem

The background to all modeling approaches of the mechanical subsystem is Newton's law as already introduced in equation (15). The product of the moment of inertia J and the angular acceleration $\ddot{\phi}$ equals the sum of the torques that act on the pivoted shaft:

$$J\ddot{\phi} = T_{el} - T_{sp} - T_f \quad (16)$$

with T_{el} , T_{sp} and T_f the electric torque, the spring torque and the friction torque, respectively. The corresponding block diagram is shown in Figure 9. As

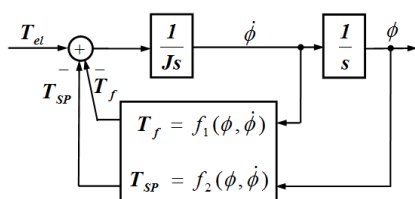


Fig. 9 Block diagram of the mechanical subsystem

the electric torque T_{el} is known from section 4 the moment of inertia J and the spring and friction torques T_{sp} and T_f have to be considered. In a first step the compounded moment of inertia J of the throttle plate, the shaft and the armature has to be identified experimentally and the identified value is

$$J \approx 30 \cdot 10^{-6} \text{kg m}^2. \quad (17)$$

In the next step the following mathematical description of the spring torque T_{sp} is introduced:

$$T_{sp} = f_2(\phi, \dot{\phi}). \quad (18)$$

This nonlinear function $f_2(\phi, \dot{\phi})$ contains a discontinuity as illustrated in Figure 10. This function describes also the behaviour at the limp-home position as presented in section 3.2.

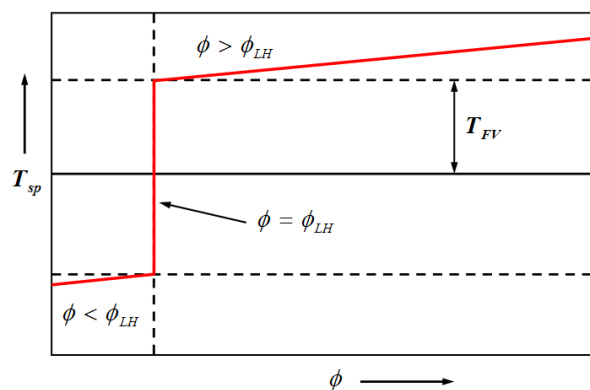


Fig. 10 Spring torque over throttle position with nonlinearity at the limp-home position

Furthermore it is assumed that both torsion springs have the same spring constant R_{F0} . If $\phi < \phi_{LH}$ the inner spring generates the spring torque T_{sp} whereas at $\phi > \phi_{LH}$ the outer spring is expanded. This can be described as

$$T_{SP} = \begin{cases} -T_{SP0} + R_F\phi & \text{if } \phi < \phi_{LH} \\ +T_{SP0} + R_F\phi & \text{if } \phi > \phi_{LH} \end{cases} \quad (19)$$

with $T_{SP0} = 0.15$ Nm. The value for the spring constant R_F is identified from an empirical equation from [16]:

$$R_F \approx \frac{Ed^4}{3667nD} \quad (20)$$

where $E = 206000$ N/mm² is the assumed elasticity modulus of the spring wire material and finally the value for the spring constant is taken as $R_F = 0.36$ Nmm/degree.

In a next step a model for the friction torque T_f has to be introduced. In the first approach it is assumed that there exists a linear relationship between the friction torque T_f and the angular velocity $\dot{\phi}$:

$$T_f = \sigma_2\dot{\phi}. \quad (21)$$

The problem to identify the friction constant σ_2 is already treated by numerous works, i.e. [12]. There is also stated that it is a complex task to find a value for this parameter and that different approaches exist. In the remainder of this paper the friction constant σ_2 remains as tuning parameter that helps to achieve an adequate compliance between the simulation model and the measurement data. The resulting value for the friction constant is taken as $\sigma_2 = 0.017$ Nms/degree.

5.2 Dahl friction model

Instead of a static feedback of the angular velocity $\dot{\phi}$ as shown in section 5.1 the friction torque T_f can also be described by means of dynamical models that consider both the static and the dynamic friction torques T_s and T_c as shown in the following equation:

$$T_f = f_3(T_s, T_c). \quad (22)$$

The characteristic for the friction torque is illustrated in Figure 11. It can be seen that before the rotation of the throttle plate begins the stiction or static friction torque T_s has to be compensated. When the throttle plate starts to rotate the dynamic friction torque T_c acts against this movement. The intersection between these two effects can be mathematically described by the nonlinear function $g(\omega_m)$. Now the problem is to find a lumped-

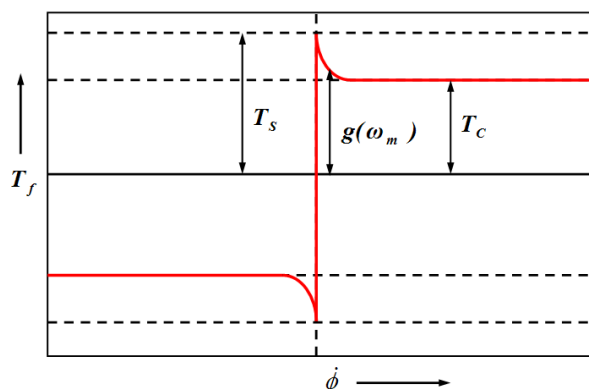


Fig. 11 Friction torque over angular velocity

parameter model for the friction torque T_f . One possibility is the well known Dahl model [13, 14, 17]. There, it is assumed that the friction torque T_f is calculated by the following equation:

$$T_f = \sigma_0 z \quad (23)$$

where σ_0 represents a model parameter for the asperity stiffness and z is the internal model state of the following first order lag:

$$\dot{T}_f = \sigma_0 \left(\omega_m - \frac{|\omega_m|}{T_c} T_f \right). \quad (24)$$

This internal model state z corresponds to the horizontal deflection of asperity contacts. In this model description the nonlinear sliding friction function $g(\omega_m)$ of Figure 11 is set to

$$g(\omega_m) = T_c = T_s. \quad (25)$$

Thus, there is no intersection between static and dynamic friction and the resulting model description becomes rather simple. A more detailed lumped-parameter model for friction modeling is introduced in the following section.

5.3 LuGre friction model

In this section the prescribed Dahl model of section 5.2 is augmented by two more physical effects [13, 14, 17]. First, the so called presliding displacement friction effect has to be introduced. This effect takes place when the throttle plate starts to rotate and it is visualized in Figure 12. It can be seen that the commanded signal of the input voltage u_{SP} is ramped up to move the throttle from standstill. Before the breakaway and real sliding occurs, the throttle moves slightly due to the compliance of asperity contacts. In terms of Figure 11 this presliding displacement effect can be seen as the impact of the nonlinear sliding friction function $g(\omega_m)$ that describes the intersection between the static friction T_s and the dynamic friction T_c .

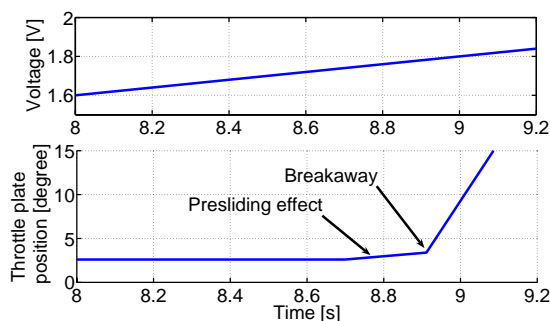


Fig. 12 Presliding displacement effect of the electronic throttle body

Additionally to the presliding displacement effect, equation (23) is augmented by a damping effect $\sigma_1 \frac{dz}{dt}$ and a viscous friction term $\sigma_2 \omega_m$. With these additional assumptions the new function for the calculation of the friction torque T_f turns into

$$T_f = \sigma_0 z + \sigma_1 \frac{dz}{dt} + \sigma_2 \omega_m \quad (26)$$

where z is again the internal model state which corresponds to the horizontal deflection of asperity contacts as shown in equation (24). The constant model parameters σ_0 and σ_1 are asperity stiffness and damping coefficients, respectively. The coefficient σ_2 represents the viscous friction. The time derivative of the horizontal deflection of asperity contacts z is assumed to be

$$\frac{dz}{dt} = \omega_m - \frac{\sigma_0 |\omega_m|}{g(\omega_m)} z. \quad (27)$$

Furthermore, the nonlinear sliding friction function $g(\omega_m)$ is modeled as

$$g(\omega_m) = T_c + (T_s - T_c) e^{-\sqrt{|\frac{\omega_m}{\omega_s}|}}. \quad (28)$$

with experimental values for the static and dynamic friction torques $T_s = 0.22$ Nm and $T_c = 0.2$ Nm.

5.4 Validation of the mechanical models

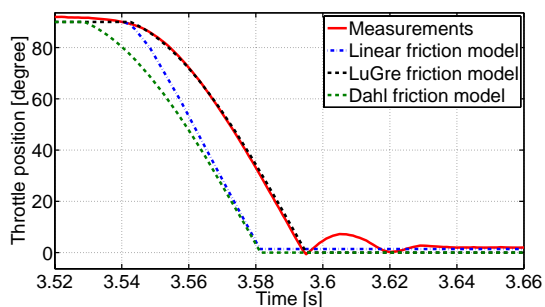


Fig. 13 Validation of the mechanical subsystem with measurement data

In this section the modeling approaches of sections 5.1, 5.2 and 5.3 are validated with measurement data. For this purpose the electronic throttle body is disengaged at $\phi = 90$ degrees and it begins to close because of the spring torque T_{sp} but the friction torque T_f decelerates this rotation. As the spring torque T_{sp} is assumed to be known from equation (18) the three modeling approaches for the friction torque T_f from sections 5.1, 5.2 and 5.3 can be adopted to the measurement data. Figure 13 illustrates that the simulation with the LuGre friction model shows the best compliance with the measurement data.

6 Overall simulation model

Sections 4 and 5 introduce each three modeling approaches for the electrical and the mechanical subsystem, respectively (Table 2):

Tab. 2 Modeling approaches for the electrical and the mechanical subsystem

Section 4.1	Linear model for the electric drive
Section 4.2	Nonlinear model for the electric drive
Section 4.3	Extended nonlinear model
Section 5.1	Linear model for the friction
Section 5.2	Dahl friction model
Section 5.3	LuGre friction model

Tab. 3 Possible combinations for the overall simulation model

	Section 4.1	Section 4.2	Section 4.3
Section 5.1	1A	1B	1C
Section 5.2	2A	2B	2C
Section 5.3	3A	3B	3C

These submodels are validated with measurements from the electronic throttle body as illustrated in sections 4.4 and 5.4. In the next step an overall simulation model has to be established. Due to several modeling approaches there exist nine possible combinations (Table 3). It can be reasoned that the combinations 1A, 1B, 1C, 2A and 3A contain at least one linear model with

a non-varying model parameter. Thus, this group of models can be taken as model description for the throttle plate behaviour at a specific operating point, that is principally for a constant input voltage u_{SP} . The remaining models contain severe nonlinearities and they are able to reproduce the throttle plate behaviour over a wide operating range. Thus, they can be taken as adequate simulation models and that helps to reduce the work on the test rig.

7 Experimental results

From Table 3 it can be seen that there exist nine possible overall simulation models. The quality of these modeling approaches has to be evaluated by the following validation process: Different steps in the input voltage $u_{SP} \in [4V, 5V, 6V]$ are applied to the electronic throttle body and the resulting throttle plate position ϕ is measured each time. This procedure is also accomplished to the nine different simulation models and conclusions are drawn. Due to spacing problems only two representative examples are shown in the remainder of this section.

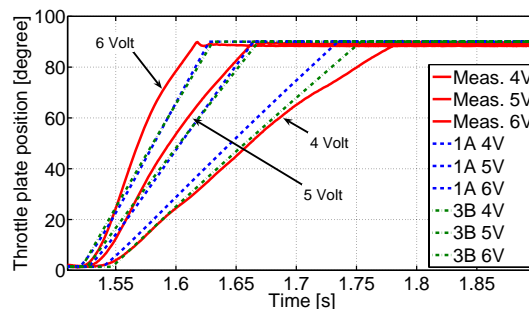


Fig. 14 Validation of the overall simulation models 1A and 3B with measurement data

In Figure 14 the overall simulation models 1A and 3B are validated with measurement data for an input voltage $u_{SP} \in [4V, 5V, 6V]$. It can be reasoned that both simulation models behave quite similar compared with the measurement data. This is particularly true for the two higher input voltages. For $u_{SP} = 4V$ the performance of the linear model 1A is lower compared to the nonlinear model. To achieve the same matching between the linear model and the measurements, i.e. two models of type 1A have to be used, one for the higher input voltages u_{SP} and one for the lower ones. With only one nonlinear model 3B the operating range is particularly extended.

Figure 15 shows a comparison between the simulation models 2B and 3B with measurement data for an input voltage $u_{SP} \in [4V, 6V]$. For the higher input voltage $u_{SP} = 6V$ it can be stated that both simulation models behave quite similar compared to the measurement data. For the lower input voltage $u_{SP} = 4V$ the electric torque T_{el} resulting from the extended nonlinear simulation model of the electric drive seems to be too high compared to the friction and spring torques

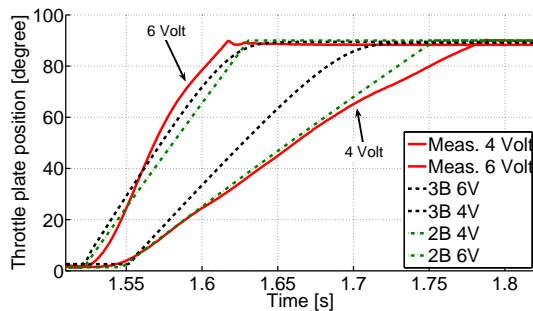


Fig. 15 Validation of the overall simulation models 2B and 3B with measurement data

T_f and T_{sp} . This is particularly true for opening angles $\phi > 20$ degrees. Hence, the aforementioned assumption that the non-magnetic shaft inside the armature can be neglected doesn't hold true for lower input voltages. Hence, future work becomes necessary in order to improve the extended nonlinear simulation model of the electric drive.

8 Conclusion and future work

This paper introduces different modeling approaches for a special design of an electronic throttle body. The electric drive of the underlying throttle body consists of a permanent magnet actuator. The aim of this paper is to give an overview of the development of existing modeling approaches. Especially, the focus lies on detailed mathematical descriptions for this new electric drive. Different simulation models both for the electric drive and the mechanical subsystem are listed, compared and validated with measurement data. If the simulation model incorporates the main nonlinearities of the electronic throttle body it will be able to cover a wide operating range realistically.

These nonlinear modeling approaches are especially interesting in the context with nonlinear control design methods. Thus, future work consists in robust nonlinear control design for the throttle plate position and it is planned to adopt nonlinear sliding mode control theory to the electronic throttle body, both in simulation and on the real plant.

9 References

- [1] J. Gerhardt, N. Benninger, and W. Hess. Torque based system structure of an electronic engine management system (me7) as a new base for drivetrain systems. In *Proceedings of the FISITA Congress*, Paris, France, 1998. Paper F98T624.
- [2] R. Rothfuss, H.-M. Heinkel, H. Schmidt, S. Stoll, and J. Winkelhake. Flatness based control of a throttle plate. In *Proceedings on the 14th MTNS*, Perpignan, France, June 2000.
- [3] D. Pavkovic, J. Deur, M. Jansz, and N. Preic. Self-tuning control of an electronic throttle. In *Proceedings of 2003 IEEE Conference on Control Applications*, pages 149–154, June 2003.
- [4] C.C. de Wit, I. Kolmanovsky, and J. Sun. Adaptive pulse control of electronic throttle. In *Proceedings of the American Control Conference*, pages 2872–2877, Arlington, VA, USA, June 2001.
- [5] Y. Pan, O. Dagi, and U. Ozguner. Variable structure control of electronic throttle valve. In *Proceedings of the IEEE International Vehicle Electronics Conference 2001*, pages 103–108, September 2001.
- [6] H.-K. Chiang and C.-H. Tseng. Implementation of a dsp-based grey integral variable structure controller for synchronous reluctance motor drive. *Electric Power Components and Systems*, 32:655–670, 2004.
- [7] C. Edwards and S.K. Spurgeon. *Sliding Mode Control, Theory and Applications*. Taylor & Francis LTD, London, 1998.
- [8] C. Rossi, A. Tilli, and A. Tonielli. Robust control of a throttle body for drive by wire operation of automotive engines. *IEEE Transactions on Control Systems Technology*, 8:993–1002, 2000.
- [9] U. Ozguner, S. Hong, and Y. Pan. Discrete-time sliding mode control of electronic throttle valve. In *Proceedings of the 40th IEEE Conference on Decision and Control*, Orlando, Florida, USA, December 2001.
- [10] O. H. Dagi, Y. Pan, and U. Ozguner. Sliding mode control of electronic throttle valve. In *Proceedings of the American Control Conference*, Anchorage, AK, USA, May 2002.
- [11] P.G. Griffiths. *Embedded Software Control Design for an Electronic Throttle Body*. Ph.D. Thesis, University of California, Berkeley, CA, USA, 2000.
- [12] J. Winkelhake. *Entwicklung eines Regelkonzepts fuer die Lageregelung einer Drosselklappe*. Diplomarbeit (in german), Institut fuer Elektrische Informationstechnik, Universitaet Clausthal, Clausthal, Germany, 2000.
- [13] J. Deur, D. Pavkovic, N. Peric, M. Jansz, and D. Hrovat. An electronic throttle control strategy including compensation of friction and limp-home effects. *IEEE Transactions on Industry Applications*, 40:821–834, 2000.
- [14] F. Altpeter. *Friction Modeling, Identification and Compensation*. Ph.D. Thesis, Ecole Polytechnique Federale de Lausanne, Lausanne, Switzerland, 1999.
- [15] D. Gerling and H. Hofmann. Single-phase reluctance actuator and single-phase permanent magnet actuator compared for low-cost applications. In *International Conference on Electrical Machines (ICEM)*, Brugge, Belgium, August 2002.
- [16] W. Matek, D. Muhs, H. Wittel, M. Becker, and D. Jannasch. *Roloff/Matek Maschinenelemente*. Viewegs Fachbuecher der Technik, 2001.
- [17] P.R. Dahl. A solid friction model. *The Aerospace Corp., El Segundo, CA, Aerospace Rep.*, TOR-0158(3107-18)-1, 1968.